5-3-2018

Mechanical Reinforcement of Polyacrylamide Hydrogels Using Pristine Single-Walled Carbon Nanotubes

Wuxiang Feng
Binghamton University--SUNY, wfeng5@binghamton.edu

MECHANICAL REINFORCEMENT OF POLYACRYLAMIDE HYDROGELS USING PRISTINE SINGLE-WALLED CARBON NANOTUBES

BY

WUXIANG FENG

BS, Wuhan Institute of Technology, 2014

THESIS

Submitted in partial fulfillment of the requirements for
the degree of Master of Science in Mechanical Engineering
in the Graduate School of
Binghamton University
State University of New York
2018

Accepted in partial fulfillment of the requirements for
the degree of Master of Science in Mechanical Engineering
in the Graduate School of
Binghamton University
State University of New York
2018

May 3, 2018

Dr. Changhong Ke, Chair and Faculty Advisor
Department of Mechanical Engineering, Binghamton University

Dr. Xin Yong, Member
Department of Mechanical Engineering, Binghamton University

Dr. Scott Schiffres, Member
Department of Mechanical Engineering, Binghamton University

Abstract

Hydrogels have great promise as an innovative biomedical material possessing many advantages such as high water content, porous structure, and excellent biocompatibility. Although hydrogels have been used to develop some successful applications, they commonly do not have sufficient mechanical strength required for artificial soft tissues. Here, the author fabricated reinforced PAAm hydrogels using single-walled carbon nanotubes as reinforcing materials. The fusion of SWCNTs and the PAAm matrix successfully generated SWCNTs/PAAm hybrid gels with improved mechanical strength. Moreover, the aqueous dispersion of SWCNTs used for engineering the hybrid gels remained excellent stability after two months. SEM images from previous research and fragments of gels after compression tests have shown that the enhancement is based on increased micro-networks in the porous structure of hydrogels and decreased stress concentration. Some phenomena, such as surface patterns, wave-like edges, and adhesiveness of gel fragments, were also mentioned and discussed.

Keywords: nanocomposite hydrogels; single-walled carbon nanotubes (SWCNTs); mechanical strength

Acknowledgment

First of all, I would like to express my gratitude to Dr. Changhong Ke for his patient guidance and warm encouragement throughout this challenging project. I would also like to thank Dr. Xin Yong, for his valuable and constructive advice during the development of this research work. My thanks are also extended to Dr. Scott Schiffres for being my committee member and taking interests in my research.

I would also like to offer my special thanks to Xiaoming Chen, Christopher Dmuchowski, Feilin Gou, Chenglin Yi, Tingting Zhang, Ohood Alsmairat, and Wenyang Qu for their helpful suggestions and generous assistance in helping me handling the instruments and revising this thesis.

Table of Contents

List of Tables

List of Figures

Introduction

Hydrogels are soft, porous, three-dimensional crosslinked polymers which can keep swollen in water and not resolved itself. Hydrogels with their advantageous characteristics such as high swelling ratio, porous framework, and high biocompatibility have been extensively used as materials for contact lenses[1], injectable implants[2], wound dressing[3], drug delivery[4], hygiene products[5], agriculture[6], scaffold in tissue engineering[7,8] and gel electrophoresis[9]. Moreover, hydrogels are considered as the only candidate for generating artificial water-rich soft tissues used as substitutes for real ones such as tendons, ligaments, cartilage, and muscle.[10] However, this is a very tough task for material scientists because hydrogels are inherently soft, weak and very sensitive to notches. Most single network hydrogels have elastic moduli and strength ranging from several hundred Pa to several hundred kPa and strain at less than 100%. The mechanical properties of single network hydrogels can be hardly compared to those of biological soft tissues. For example, the elastic modulus of polyrotaxane gel that immersed in different solutions ranged from 0.5 kPa to 2 kPa.[11] Compressive tests of PEG hydrogels showed that its elastic modulus and failure stress could reach as high as 230 kPa and 180 kPa.[12] The compressive failure stress and strain of agarose gel were reported to be 606 kPa and 0.36, respectively, when the concentration of agarose solution used for this test was 10 wt%[13]. In contrast to single network gels, the mechanical properties of soft tissues are much more superior. For example, cartilage with 68-85 wt% water exhibits Young's moduli of 1-10 MPa (tension) and 1 MPa (compression), yield strength of 3 MPa and

ultimate tensile strength ranging from 10-35 MPa.[10,14] Ligament, containing 60-80% water of its wet weight, shows Young's modulus of 1.2-1.8 GPa, ultimate failure stress of 50-150 MPa (tension) and ultimate failure strain of 13-18%.[14] Thus, methods to strengthen the mechanical properties of hydrogels without compromising their beneficial qualities are desirable.

Incorporation of CNTs within the hydrogels is one of the methods that can significantly improve the mechanical properties of hydrogels. For example, Liu et al. reported that the P(AM-co-SMA) hydrogels infused with MWNTs-COOH exhibited considerable compressive strength and improved recoverable strain. In compression tests, the P(AM-co-SMA)/MWNTs-COOH nanocomposite hydrogels in buffer solutions of PH=1.4 with 1.5 wt% MWCNTs showed a maximum increase of 60% in failure stress[15]. Chatterjee et al. investigated the mechanical strength of chitosan (CS) hydrogel beads impregnated with MWCNTs and found the maximum compressive force the hydrogel beads could withstand increased from 1.87 N for neat CS hydrogel to 7.62 N when only 0.01 wt% MWCNTs were added into the CS matrix.[16] Wang et al. also reported increases of 93% and 99% for the tensile modulus and strength of CS hydrogel, respectively, by infusing 0.8 wt% MWCNTs into the CS matrix.[17] Dong et al. reported the fabrication of PAMPS/PAAm/CNTs nanocomposite DN hydrogels. The nanocomposite hydrogels reinforced by MWCNTs without organic modification showed superior mechanical properties, and their compressive modulus and fracture stress were about 4.5 times and 4 times as high as that of neat hydrogels respectively.[18] Shin et al. engineered MWCNT-embedded GelMA hydrogel sheets. They found that the incorporation of 3 mg/ml MWCNTs led to the compressive modulus increasing from 10 kPa to 32 kPa.[19] However,

most of the research used MWCNTs as nano-fillers which are easier to disperse in water but are weaker in mechanical strength than SWCNTs. Although SWCNTs possess the best specific strength of up to 48,000 $kN \cdot m/kg$, the strong van der Waals interactions ($\sim 40\ k_B T/nm$) between adjacent SWCNTs make them difficult to disperse.[20,21] But if this problem can be overcome, a significant leap on the mechanical strength of nanocomposite materials may be realized. Also, the effectiveness of de-agglomeration and the homogeneity of CNTs, which play essential roles in enhancing the mechanical properties of hybrid hydrogels, were not sufficiently studied in previous research. Although some methods such as analysis of TEM and SEM images were performed to investigate them, these images can only illustrate the local condition of nanocomposite gels.

To create a CNT reinforced nanocomposite hydrogel, the author utilized polyacrylamide (PAAm), which has been a general medium used in almost all electrophoretic methods. PAAm is of exceptional promise for research areas, such as enzyme immobilization[22], carriers for drug delivery[23], smart materials[24], and extracorporeal toxin removal modalities[25], owing to its non-toxic and non-biodegradable qualities. PAAm gels, formed by copolymerization of acrylamide and N,N'-methylene-bis-acrylamide (BIS), are transparent synthetic hydrogels. The monomers, acrylamide (AAm), are polymerized by vinyl addition process initiated by free radical-generating agents, ammonium peroxydisulfate (APS) and N,N,N',N'-tetramethyl-ethylenediamine (TMEDA). TMEDA also serves as a catalyst that speeds up the formation of free radicals. Free radicals then turn the monomers into more free radicals thus elongating the polymer chains which are randomly cross-linked by the crosslinking agents, BIS.

In this thesis, the author reports nanocomposite hydrogels with pristine SWCNTs homogeneously incorporated into PAAm matrix, demonstrating significant improvement in mechanical strength compared with neat PAAm hydrogel. The compressive test results illustrate that the compressive modulus, a critical parameter for tissue engineering[19,26], increased from 13.2 kPa for neat PAAm gels to as high as 57.4 kPa for SWCNTs/PAAm hybrid gels with a concentration of SWCNTs at 0.5 mg/ml. This concentration is lower compared with previous research using MWCNTs as nano-fillers that obtained similar improvement in mechanical strength[18,19]. The author first prepared the dispersion of SWCNTs following a sequence of sonication, centrifugation, and filtration. Then an estimation of the concentration of individual SWCNTs in the dispersion was conducted. The dispersion of SWCNTs remained remarkably stable and homogeneous after two months storage. The author next incorporated the SWCNTs into the PAAm gel matrix and investigated the mechanical properties of the hybrid hydrogels by compression tests. The compression tests revealed significantly improved compressive modulus, fracture stress, toughness but diminished fracture strain. This thesis reviews the toughening mechanism of the hybrid hydrogel base on SEM images and fragments of hydrogels. Some phenomena observed in the experiment are also mentioned and discussed.

Experiment

Materials

Acrylamide (AAm, 99.9%), N,N'-methylene-bis-acrylamide (BIS, 99%), ammonium peroxydisulfate (APS, 98%), N,N,N',N'-tetramethyl-ethylenediamine (TMEDA, 99%) , sodium dodecylbenzene sulfonate (NaDDBS, 99%) were purchased from VWR International, Inc. Single-walled carbon nanotubes (SWCNT, 1-2 nm in diameter, 1.1 nm in average diameter, 5-30 μm in length, 98% in purity) were purchased from US Research Nanomaterials, Inc. All materials were used as received.

The weight ratio of SWCNTs to NaDDBS

Olga et al. reported that once NaDDBS molecules have saturated the surface of the nanotubes, the additional NaDDBS surfactant is unnecessary and may act as an impurity in the solution.[27] By a number of trials, it was found that the weight ratio of SWCNTs to NaDDBS at 1:4 can disperse the SWCNTs effectively, although Islam et al. reported that the optimal ratio was 1:10.[18] Higher weight ratio might induce foaming of surfactants that compromises the dispersion of SWCNTs, while lower weight ratio is not sufficient to disperse the nanotubes effectively.

The aqueous dispersion of SWCNTs

SWCNTs (0, 5, 10, 20 mg) and NaDDBS with the weight ratio of 1:4 respectively were added to 20 ml distilled water. The mixture of SWCNTs, NaDDBS,

and distilled water was sonicated by horn sonication (20% amplitude, 2 sec on and 1 sec off) for 15 min in an ice bath (Figure 1). The reason for using 20% amplitude is that the cavitation phenomenon may be too strong above this value, generating intense shock waves and foam of the surfactant.[28–30]

(a)

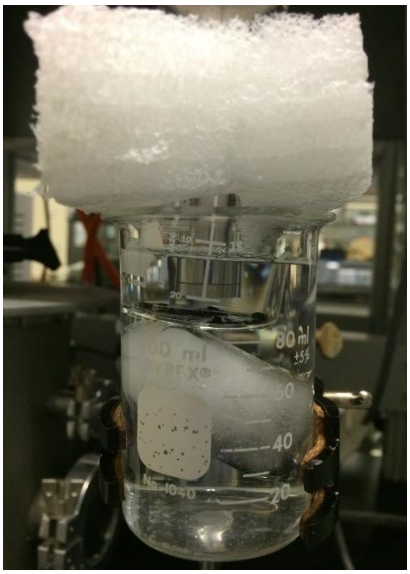

(b)

Figure 1. (a) Branson S-450 digital ultrasonic homogenizer and 13mm tapped horn with a flat tip. (b) The dispersion was put in a beaker floating on the iced water.

To examine the degree of the de-agglomeration of the SWCNTs after sonication, we took a droplet of dispersed SWCNTs out of the beaker and dropped it into a glass of distilled water. If there were visible bundles of SWCNTs, it was decided that the suspension need more sonication until no bundles can be observed (Figure 2). This direct and straightforward testing method is named as the degree of CNTs de-agglomeration test (DCDT) in this thesis. Due to the nanoscopic scale of the diameter of SWCNTs, DCDT is inaccurate, but it can show a rough degree of the de-agglomeration intuitively and quickly.

The suspension was subsequently centrifuged at a speed of 2000 r/min for 30 min.[31] Finally, the mixture was filtered by a 325 mesh (44 μm) stainless steel screen filter to remove the sediment that made up of bundles of SWCNTs. After filtration, the filter was gently washed with distilled water to get rid of residual NaDDBS and then dried in a vacuum box at 100℃ to remove residual water.[32] The weight of the sediment of SWCNTs bundles can be determined by subtracting the weight of clean filter from the weight of sediment and filter after drying. The percentage of individual SWCNTs can be expressed as

$$\%\mathrm{D} = \frac{M_{cnt} - (M_{f'} - M_f)}{M_{cnt}} 100\%$$

where %D is the percentage of individual SWCNTs in the dispersion, M_{cnt} is the weight of total SWCNTs, $M_{f'}$ is the weight of sediment and filter after drying, and M_f is the weight of the clean filter.

We obtained that the %D was approximately 52%, 47%, 55% respectively for dispersion with 5, 10, 20 mg SWCNTs added initially. Here, we assumed that %D for all three dispersions are 50% for ease of calculation. The concentration of the SWCNTs in

the final four aqueous dispersion was 0, 0.125, 0.25, 0.5 mg/ml respectively.

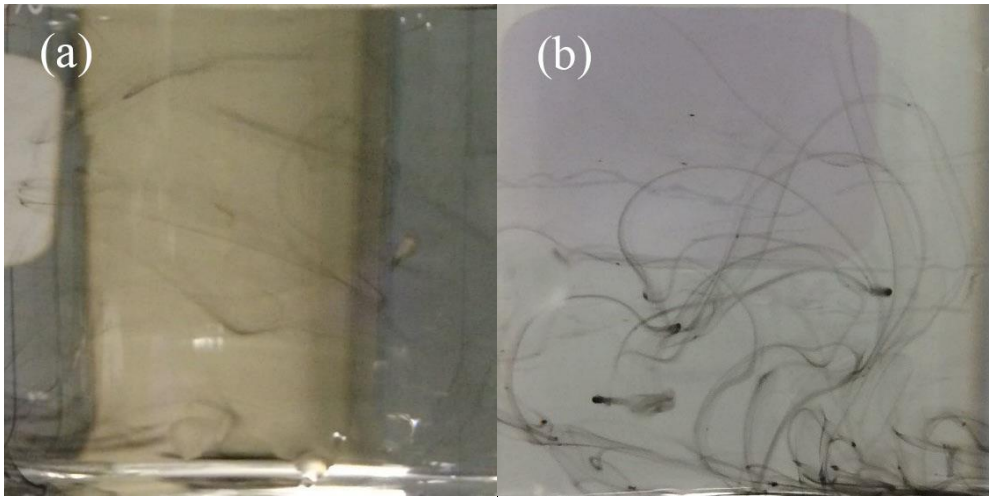

Figure 2. The diffusion of a droplet of the dispersion in the water illustrates the degree of de-agglomeration of SWCNTs. (a) Well-dispersed SWCNTs (b) Agglomerated SWCNTs

SWCNTs/PAAm hydrogels

The crosslinking agent BIS (25 mg) was first added into 10ml aqueous dispersion of SWCNTs (varied at 0, 0.125, 0.25, 0.5 mg/ml) and mildly sonicated (10% amplitude) until it fully dissolved in the dispersion. Subsequently, the monomer AAm (1g), the initiator APS (10 mg) and the accelerator TMEDA (10μl) were successively added to the dispersion in an ice bath.[33] After being vigorously stirred for 15 min, the mixture was distributed into vials with 1 ml mixture in each of them. The vials were put in ambient environment for 3 min to equilibrate to room temperature (23-25 ℃) and then degassed in a vacuum box under a pressure of 23 Torr or lower for 30 min.[34] Lids were instantly closed after the vials were taken out of the vacuum box to keep the hydrogels from being contaminated and dehydrated. The as-prepared hydrogels (Figure 3) were left alone for at least 12 hours in the vials to complete the polymerization.[34] The formulations of SWCNTs/PAAm hydrogel are listed in Table 1.

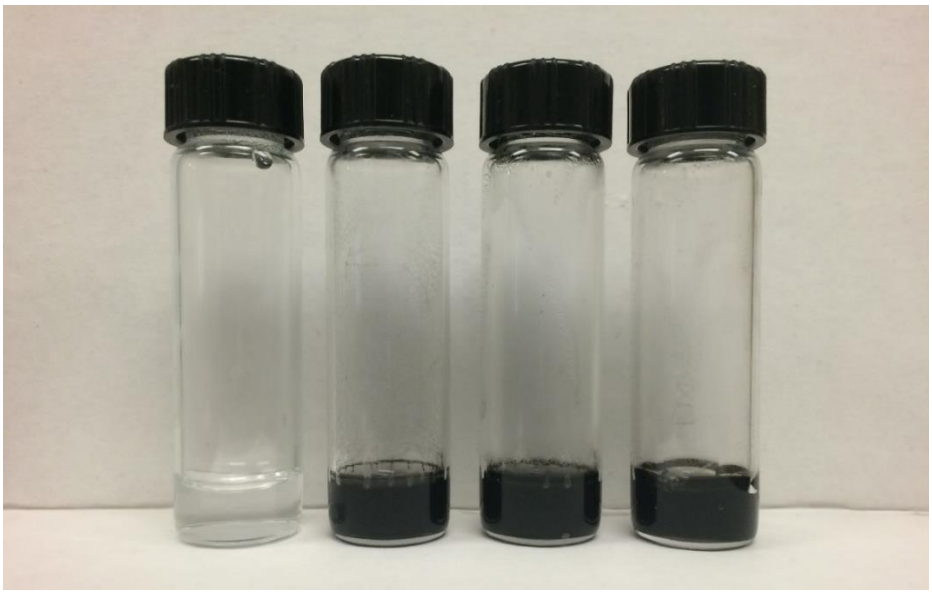

Figure 3. As-prepared hydrogel samples with a concentration of SWCNTs varied at 0, 0.125, 0.25, 0.5 mg/ml respectively.

Table 1. The formulations of SWCNTs/PAAm hydrogels

Hydrogels	C_{CNTs} (mg/ml)	C_{NaDDBS} (mg/ml)	C_{PAAm} (mg/ml)	C_{BIS} (mg/ml)	C_{APS} (mg/ml)	C_{TEMDA} $(\mu l\ /\ ml)$
CNT_0	0	0	100	2.5	1	1
$\mathrm{CNT}_{0.125}$	0.125	1	100	2.5	1	1
$\mathrm{CNT}_{0.25}$	0.25	2	100	2.5	1	1
$\mathrm{CNT}_{0.5}$	0.5	4	100	2.5	1	1

Compression test

A universal testing machine (ADMET eXpert4000 with MTESTQuattro) was used for compression tests at room temperature (Figure 4). The cylindrical samples were taken out of the vials right before use and then immersed in distilled water for several seconds. The compression tests for all samples were finished within 4 min so that they

can remain their original hydrated conditions at the end of the tests. Since all samples were polymerized out of 1ml mixture in the vials, they have same dimensions. Each of the cylindrical samples with 14.3 mm in diameter and 6.2 mm in height was put on the lower plate and compressed by the upper plate connected with a 100 lbf (444.8 N) load transducer (Figure 5). The strain rate for the compression tests was 2 mm/min. The compression stopped as soon as the stress dropped by 15% concerning the peak stress. For each group of hydrogels with the same concentration of SWCNTs, eight samples were produced for compression tests from which at least three samples obtained valid experimental data for data processing.

Figure 4. ADMET eXpert4000 universal testing machine with the MTESTQuattro materials testing system was used for the compression tests.

The compressive stress σ_c was approximately determined by engineering stress:

$$\sigma_c = F/\pi R^2$$

Where F is the compressive force applied to the specimen, R is the radius of the as-prepared specimen.

The compressive strain ε, defined as engineering strain, was determined by the ratio of the change in the height of specimen to the original height of the specimen:

$$\varepsilon = (h_0 - h)/h_0$$

Where h_0 is the original height of the specimen, h is the height of the specimen under compression.

The Young's modulus for compression was defined as the slope of the stress-strain curve at ε between 0 and 0.1. The toughness was determined by the area under the compressive stress-strain curve.

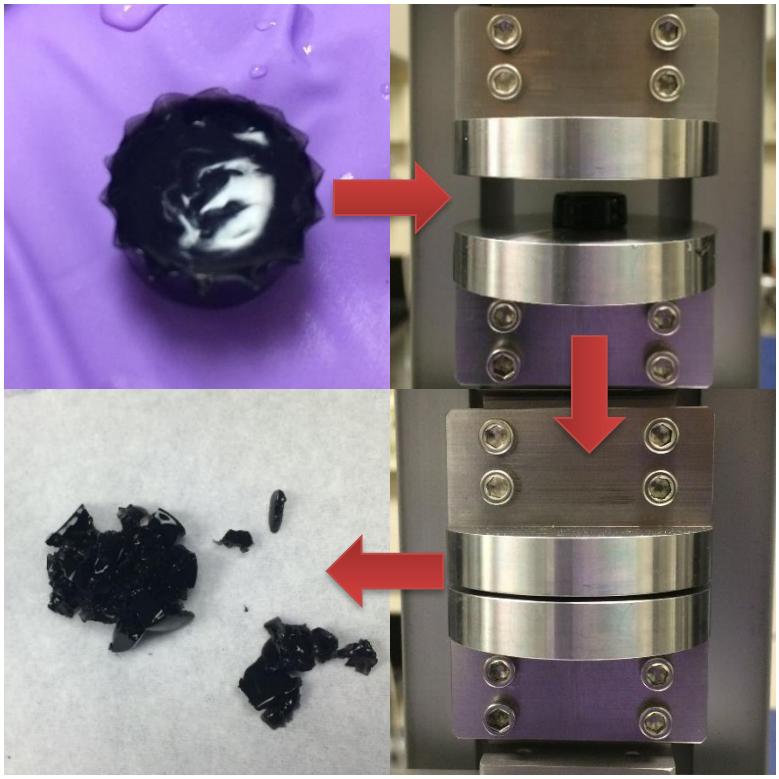

Figure 5. Compression tests for SWCNTs/PAAm nanocomposite hydrogels.

Results and Discussion

The stability of aqueous dispersion of SWCNTs

The stability of aqueous dispersion of SWCNTs is an important parameter that affects the mechanical strength of nanocomposite hydrogels. Although individual SWCNTs have exceptional axial mechanical strength and aspect ratios, which we want to take full advantage, the agglomeration of SWCNTs that generates bundles of CNTs results in diminished aspect ratios and mechanical strength of only a few GPa[35]. We noticed that the well-dispersed SWCNTs in the dispersion processed only by sonication re-agglomerated easily under slight vibration or temperature changes, making fabrication of homogenous SWCNTs/PAAm hydrogels nearly impossible. However, the dispersion with a concentration of SWCNTs at 0.5 mg/ml prepared in our experiment processed by sonication, centrifugation and filtration can still keep stable after two months, demonstrating few sediment in the dispersion (Figure 6). Moreover, no sediment or bundles of CNTs were observed in the aqueous mixture consisting of AAm, BIS, APS, TMEDA, and dispersed SWCNTs after being treated with mixing, stirring, and sonication by DCDT. Therefore, the dispersion of SWCNTs prepared by methods above can be used to fabricate homogeneous SWCNTs/PAAm hydrogels.

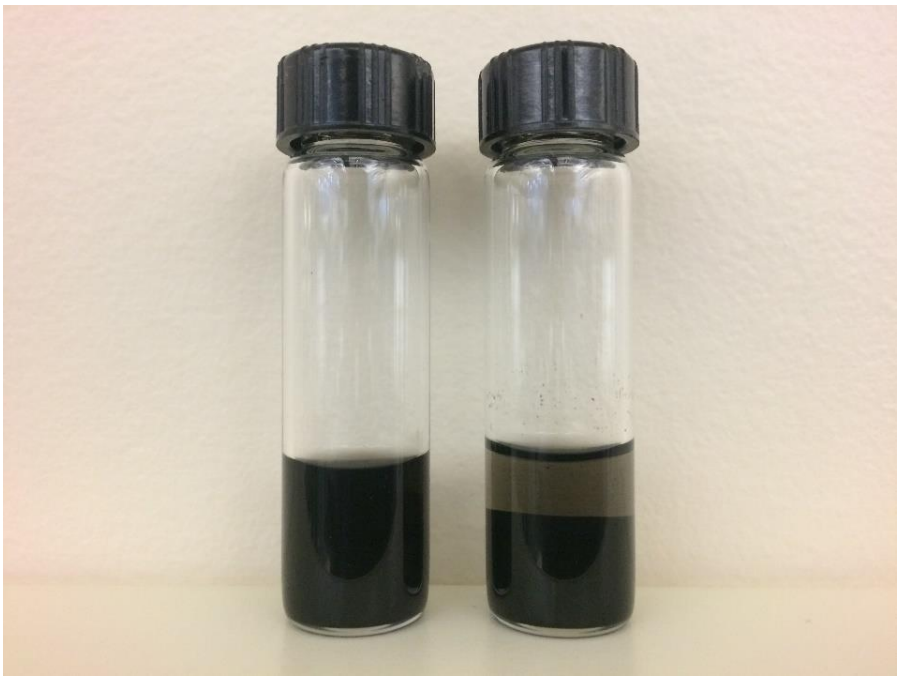

Figure 6. Two vials of 0.5 mg/ml dispersion of SWCNTs were put alone for two months. The left one was treated with sonication, centrifugation, and filtration. The right one was treated only by sonication.

Compressive Behavior

The compressive stress-strain curves are shown in Figure 7, which demonstrate the tendency of enhancing mechanical strength with the addition of SWCNTs.

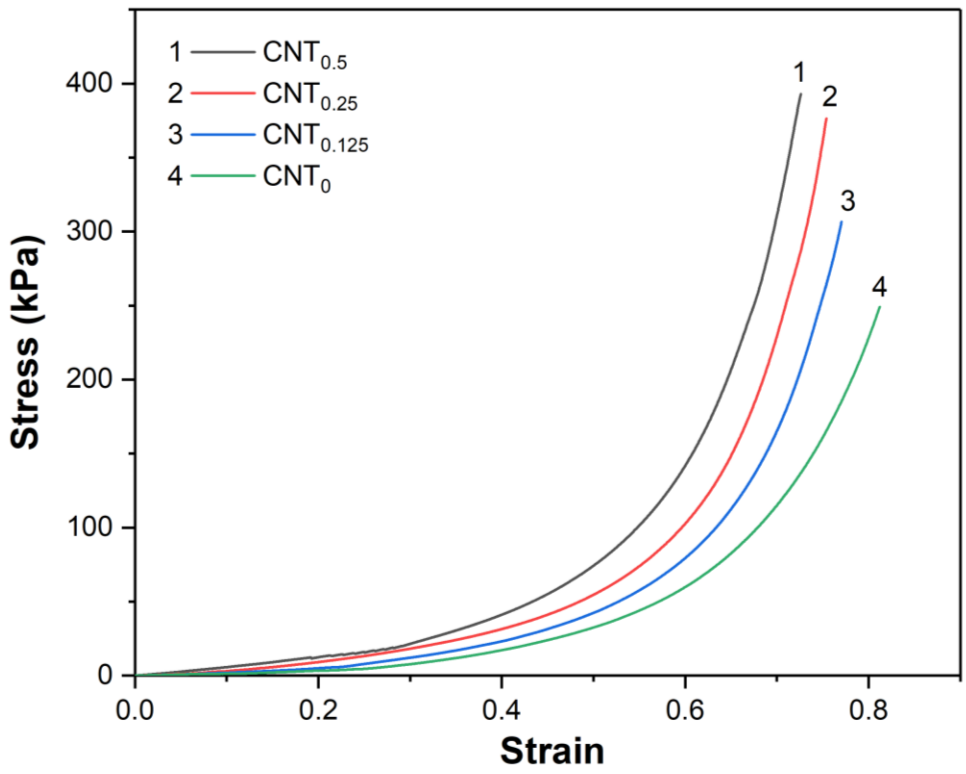

Figure 7. Stress-strain curves for SWCNTs/PAAm hydrogels with varied concentrations of SWCNTs.

The experimental data of compressive modulus, fracture strain, fracture stress, and toughness for neat and nanocomposite hydrogels are listed in Figure 8 and Table 2. Apparently, the incorporation of SWCNTs into hydrogels led to an increase in Young's modulus, fracture stress, and toughness, yet a decrease in fracture strain. The Young's modulus of SWCNT-filled nanocomposite hydrogels (SWCNTs, 0.5mg/ml) was 57.4 ± 4.7 kPa, leading to more than fourfold increase, compared with neat PAAm hydrogels (13.2 ± 2.1 kPa). The fracture stress increased by 58%, from 249.1 ± 15.8 kPa for neat PAAm hydrogels to 393.1 ± 27.0 kPa for $CNT_{0.5}$. The toughness also increased by 44% from 36.6 ± 3.4 KJ/m^3 for CNT_0 to 52.3 ± 4.0 KJ/m^3 for $CNT_{0.5}$. However, the fracture strain slightly declined by 11% from 0.81 for neat PAAm gels to 0.72 for $CNT_{0.5}$.

Table 2. The mechanical properties of SWCNTs/PAAm hydrogels with varied concentrations of SWCNTs

Hydrogels	Compressive modulus (kPa)	Fracture stress (kPa)	Fracture strain	Toughness (KJ/m^3)
CNT_0	13.2 ± 2.1	249.1 ± 15.8	0.81 ± 0.05	36.6 ± 3.4
$CNT_{0.125}$	19.9 ± 3.3	306.6 ± 23.5	0.77 ± 0.07	39.6 ± 5.3
$CNT_{0.25}$	31.0 ± 3.5	376.4 ± 31.3	0.75 ± 0.06	47.5 ± 4.8
$CNT_{0.5}$	57.4 ± 4.7	393.1 ± 27.0	0.72 ± 0.04	52.3 ± 4.0

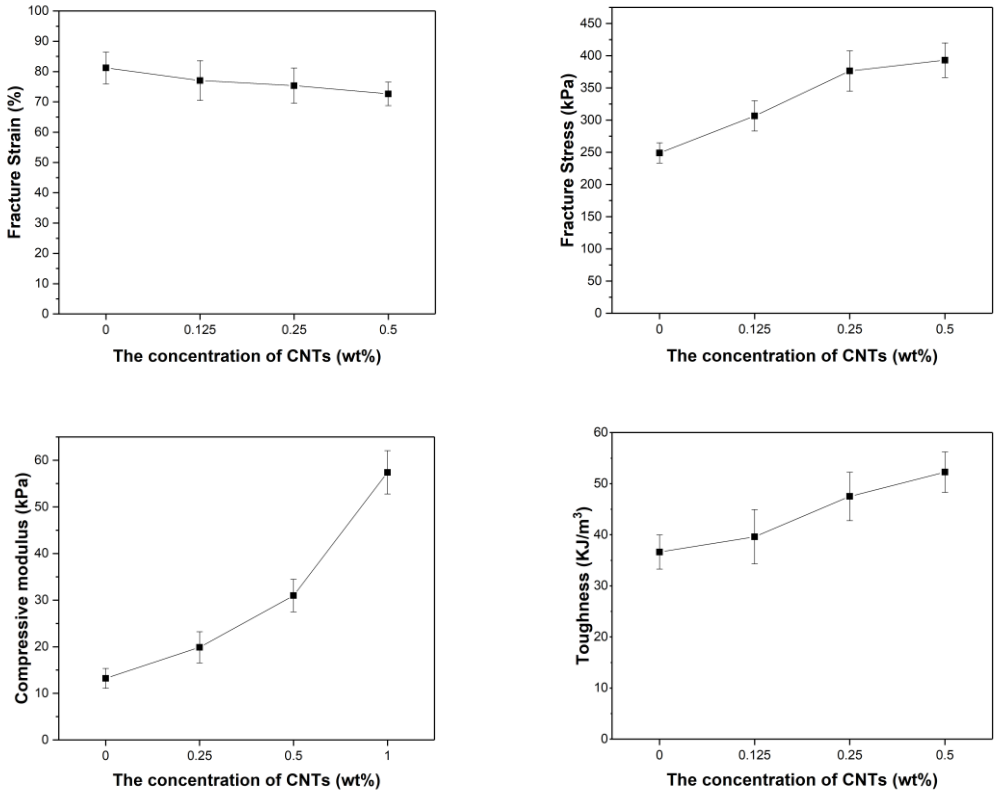

Figure 8. The mechanical properties of SWCNTs/PAAm hydrogel samples with varied concentrations of SWCNTs

Toughening mechanism

To understand the toughening mechanism of SWCNTs/PAAm hybrid gels, it is

necessary to know the reasons for the weak mechanical strength of neat PAAm gels.

One reason is the scant friction between polymer chains due to the low concentrations of polymer chains and the mesh structure of hydrogels (Figure 9).[10,36] Gong et al. presented double network gels prepared by two different polymer monomers polymerized in proper order, exhibiting extraordinary mechanical strength comparable to real soft tissues.[10] The second polymer network brings about more friction between polymer chains and increases the concentration of polymer chains, thus reinforcing the mechanical strength of the hybrid gels.

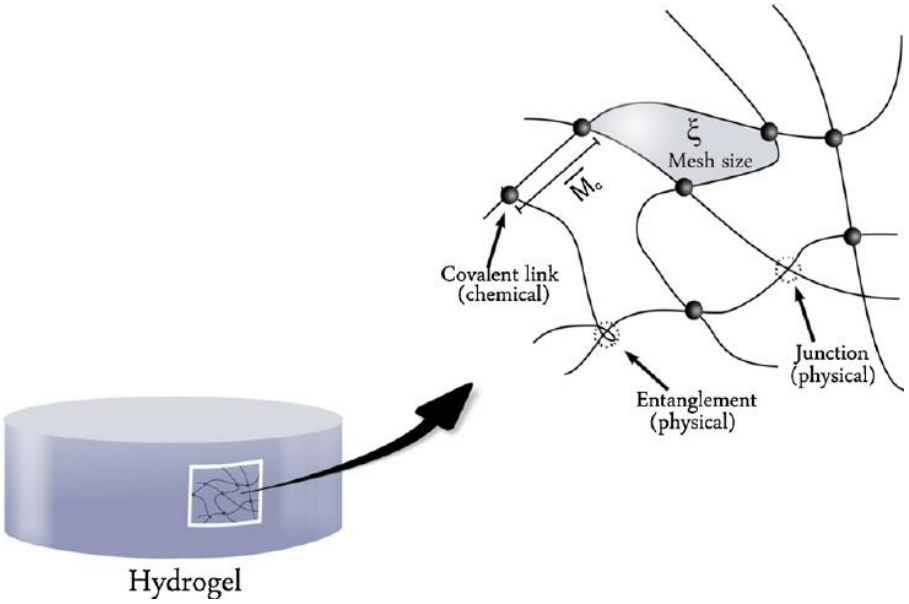

Figure 9. The structure of a crosslinked hydrogel with mesh size ξ. (Reproduced from literature.[36])

Another reason is the heterogeneities of the network of hydrogels. The various length of chains engenders stress concentrating on the shortest chain.[37,38] This could be verified by some unexpectedly low fracture stress and strain of PAAm gels observed in the compression tests. The heterogeneities can be ameliorated by improved experimental methods, such as more stirring during the gelation, but they can't be entirely avoided.

The PAAm gels we made (10 %T, 1 %C) possessing a compressive modulus of 13.2 kPa can be regarded as relatively homogeneous gels according to the experimental data showed in Figure 10.[39]

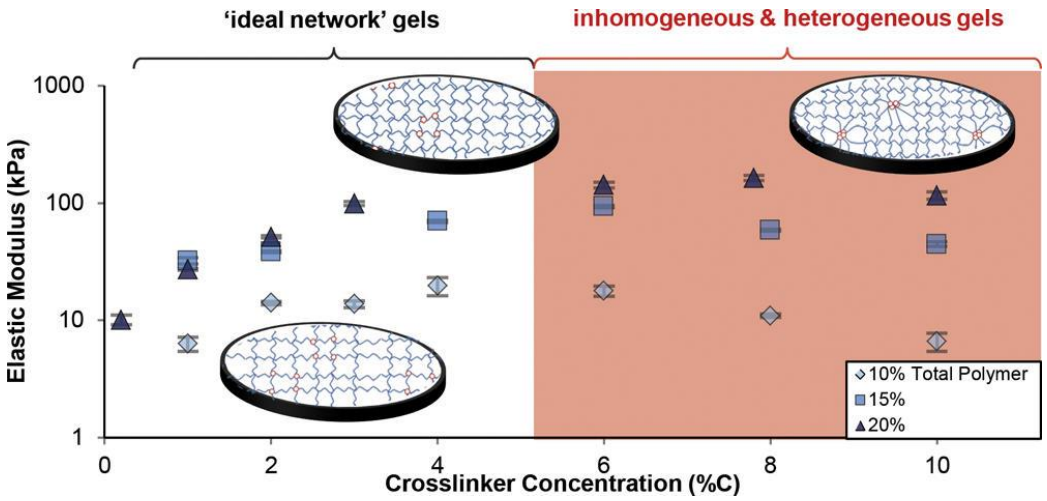

Figure 10. The elastic modulus of PAAm gels with different total polymer content (%T) and crosslinking agent content (%C). (Reproduced from literature.[39])

Here, we speculate that the infused SWCNTs can interact with PAAm networks, leading to more friction and entanglement. Figures 11 and 12 show the SEM images of the microstructure of PAMPS/PAAm double network hydrogels incorporated with pristine MWCNTs, which may also be useful for illustrating the microstructure of SWCNTs/PAAm hybrid gels. (In Figures 11 and 12, CNTs-α indicates the weight ratio of MWCNTs to AMPS is α wt%. The concentration of AMPS is 1 mol/L. Therefore, the concentration of CNTs of 4 specimens is approximately 0, 1, 2, 8 mg/ml respectively.) As is shown in the images, the micro-networks in the pores increases with the incorporation of MWCNTs. These micro-networks may contribute to energy dissipation and less stress concentration. A few CNTs bundles were also observed to exist on the pore wall, which may lead to a more rigid pore structure resulting from friction between CNTs and polymer chains.

The SWCNTs may also reduce the heterogeneity of the network of the hydrogels. We found that the sizes of the fragments of hybrid gels after compression tests are much smaller than those of neat PAAm gels (Figure 13, Figure 14), which may be an indication of a more homogeneous porous structure of the hybrid gels.

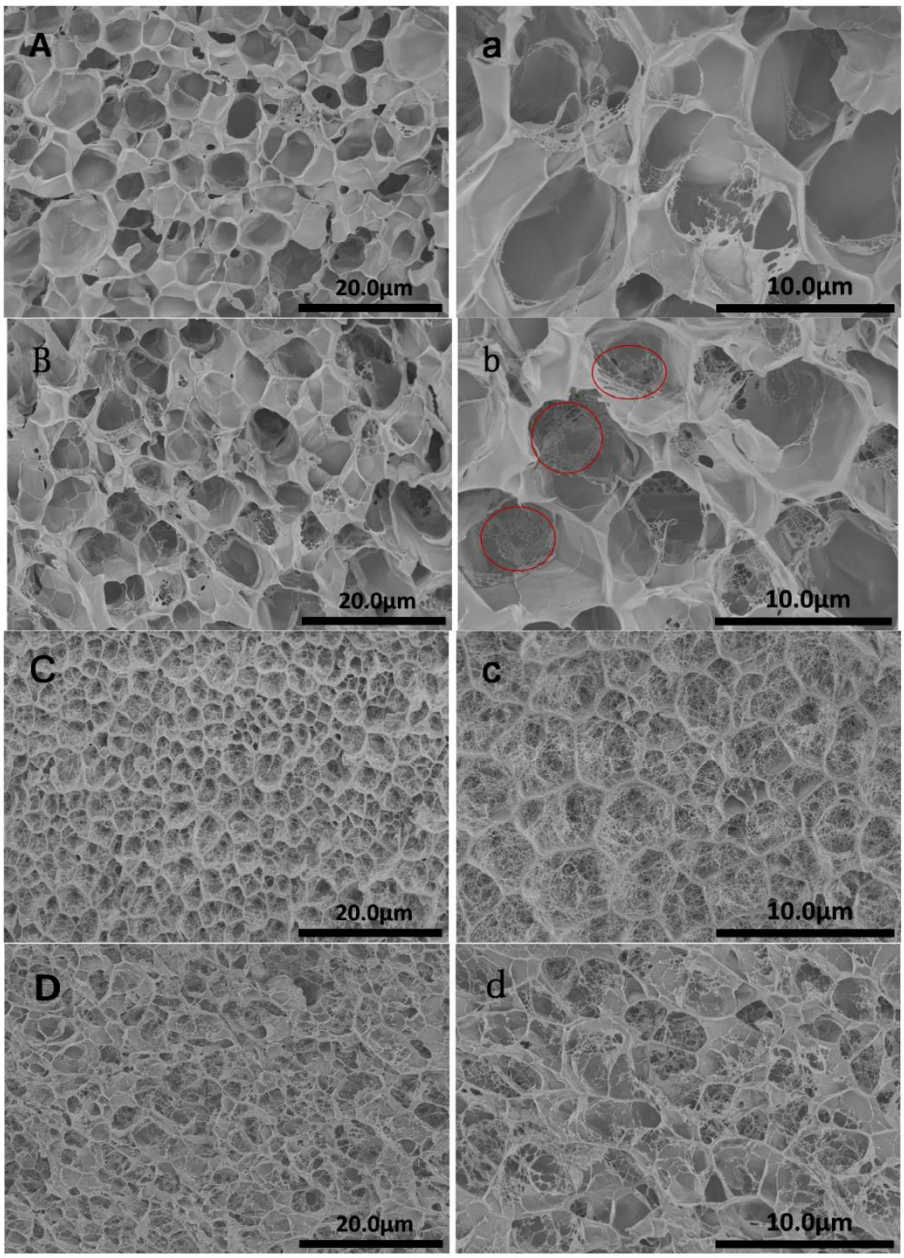

Figure 11. The SEM images of nanocomposite PAMPS/PAAm/MWCNTs double network hydrogels (A,a) CNTs-0; (B,b) CNTs-0.5; (C,c) CNTs-1 and (D,d) CNTs-4. (Reproduced from literature.[18])

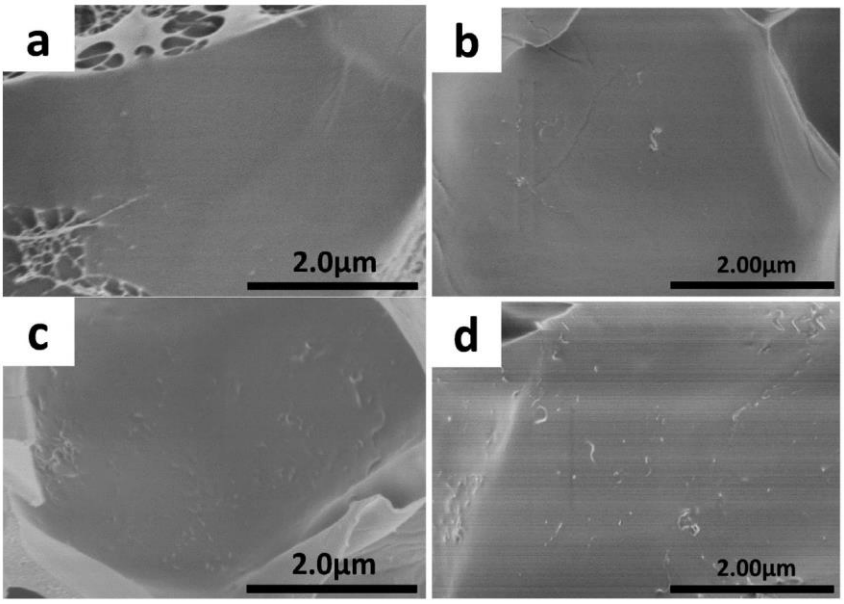

Figure 12. The SEM images of pore wall for nanocomposite PAMPS/PAAm/MWCNTs double network hydrogels (a) CNTs-0; (b) CNTs-0.5; (c) CNTs-1; and (d) CNTs-4. (Reproduced from literature.[18])

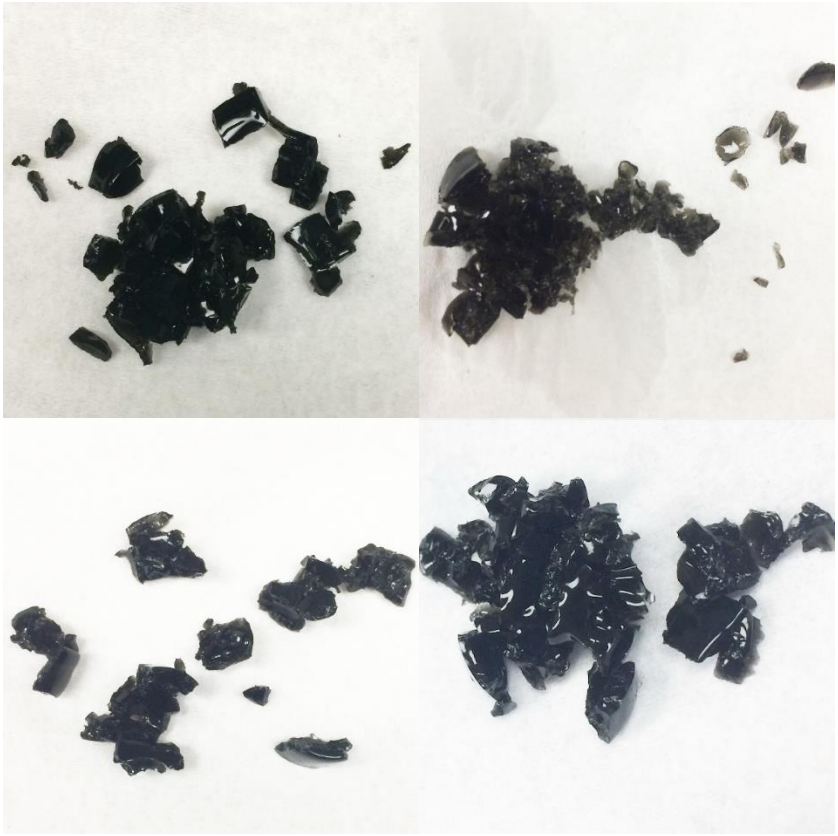

Figure 13. Fragments of SWCNTs/PAAm hybrid gels after compression tests.

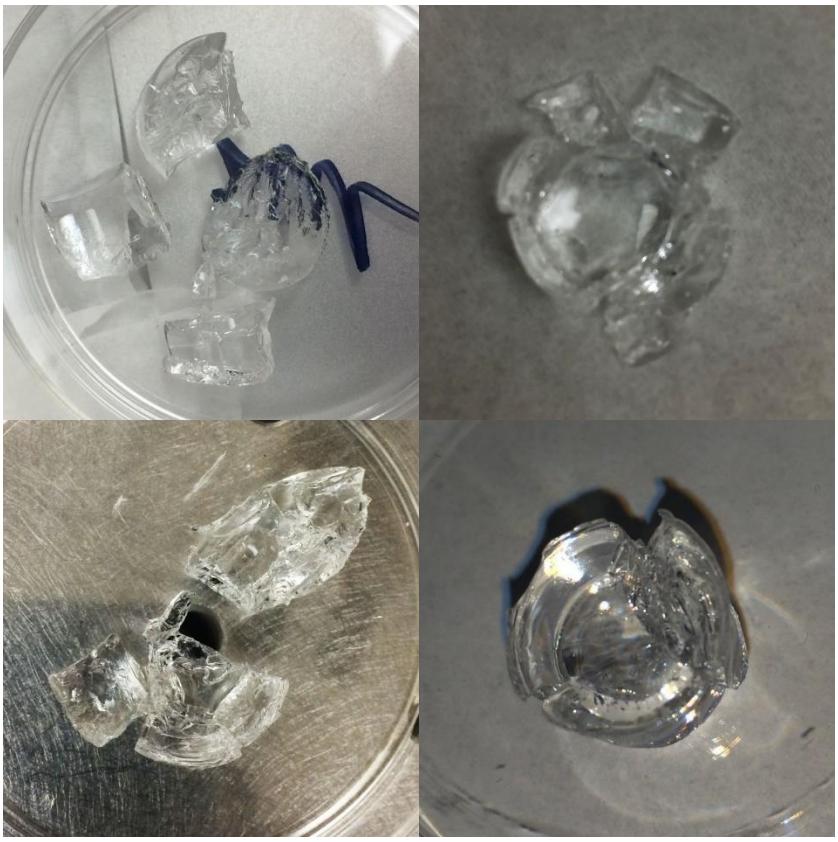

Figure 14. Fragments of neat PAAm gels after compression tests.

Two exceptionally reinforced samples

We noticed that two specimens of SWCNTs/PAAm nanocomposite hydrogels demonstrated more pronounced enhancement of fracture stress or fracture strain. Due to their unusual performance, their experimental results were excluded from the valid data. However, the fact that their performance was observed in the experiment made them deserve our attention. For example, one specimen of $CNT_{0.125}$ gels did not break until the compressive stress reached as high as 1 MPa, which was more than twice of what achieved by $CNT_{0.5}$ gels. It also demonstrated an extraordinary toughness that was three times higher than that of neat PAAm gels. Its fracture strain and compressive modulus also reached a relatively high value of 0.84 and 38.7 kPa respectively. Another specimen

of $CNT_{0.5}$ gels with the compressive modulus of 16.8 kPa withstood an outstanding compressive strain as high as 0.98 when the compressive stress was 450 kPa (Figure 15). The mechanical properties of these two specimens and neat PAAm hydrogels are listed in Table 3.

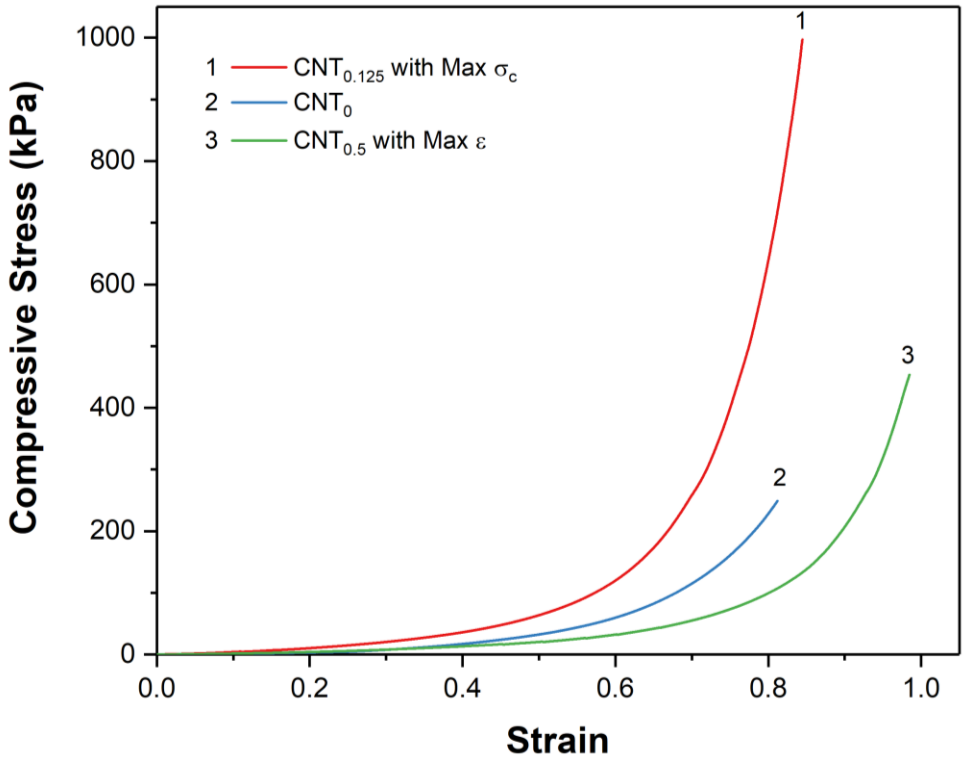

Figure 15. The stress-strain curves of neat PAAm gels, a sample of $CNT_{0.125}$ with maximum fracture stress, and a sample of $CNT_{0.5}$ with maximum fracture strain

Table 3. The mechanical properties of neat PAAm hydrogels, a sample of $\mathbf{CNT_{0.125}}$ with maximum fracture stress, and a sample of $\mathbf{CNT_{0.5}}$ with maximum fracture strain

Hydrogels	Compressive modulus (kPa)	Fracture stress (kPa)	Fracture strain	Toughness (KJ/m^3)
CNT_0	13.2 ± 2.1	249.1 ± 15.8	0.81 ± 0.05	36.6 ± 3.4
$CNT_{0.125}$ $(max\ \sigma_c)$	38.8	997.2	0.84	113.9
$CNT_{0.5}$ $(max\ \varepsilon)$	16.8	453.6	0.98	58.6

The exceptional mechanical properties possessed by these specimens indicate the promisingly potential on reinforcing the mechanical strength of SWCNTs/PAAm nanocomposite hydrogels. We hypothesize that the reasons for the performance of the two specimens are as follows.

1. The SWCNTs are more homogeneously distributed in these two specimens, leading to more effective energy dissipation and less stress concentration.
2. The SWCNTs in these two specimens have better alignment in specific directions that may be especially beneficial in the compression tests.
3. Although the group of hydrogels with the same concentration of SWCNTs was prepared with the same batch of the aqueous dispersion of SWCNTs, the degree of de-agglomeration of SWCNTs in the dispersion has not been examined by specialized instruments other than DCDT. That being said, there may be more individual SWCNTs in these specimens than others, leading to a more extensive contacting surface area for the interaction between SWCNTs and PAAm matrix.

Phenomena Observed in the Experiment

The surface patterns of neat PAAm gels

When preparing the neat PAAm gels, it was found that some stable and systematically arranged patterns sometimes appeared on the top surface of the cylindrical samples of PAAm gels after they were taken out of the vacuum box. These patterns are grooves on the surface and showed a good recoverability after deformation (Figure 16). Gel samples with same and different sizes were made and showed similar pattern units such as T-shaped and Y-shaped unit. However, no sample showed the same surface pattern as other samples (Figure 17, Figure 18). Tanaka first reported these patterns on the hydrogels in 1987 that were then further investigated by a few types of research.[40] For example, Guvendiren et al. reported similar surface patterns on PHEMA films confined on a flat substrate.[41] By controlling the modulus gradient or osmotic pressure with depth, four typical surface patterns were captured. The surface patterns were considered to be generated by a buckling effect due to a mismatch between moduli in a bilayer film. However, the method we used to form the surface patterns was distinct from others. For example, the bilayer film is not required in our method, and the surface of the PAAm gels does not need to be immersed in water to start the formation of the patterns. Accordingly, the method we used may serve as an alternative way to create surface patterns in the future.

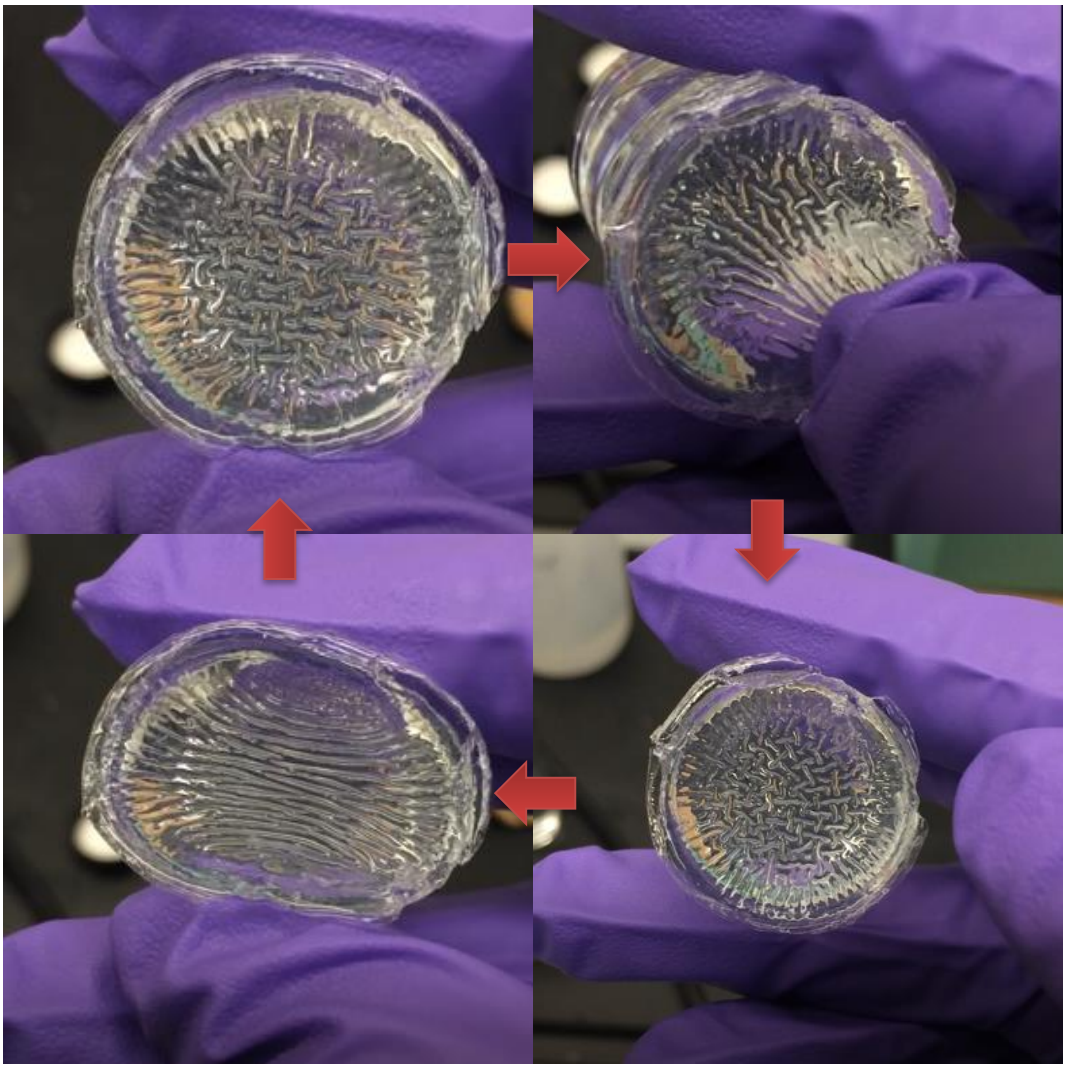

Figure 16. The patterns showed good recoverability after deformation.

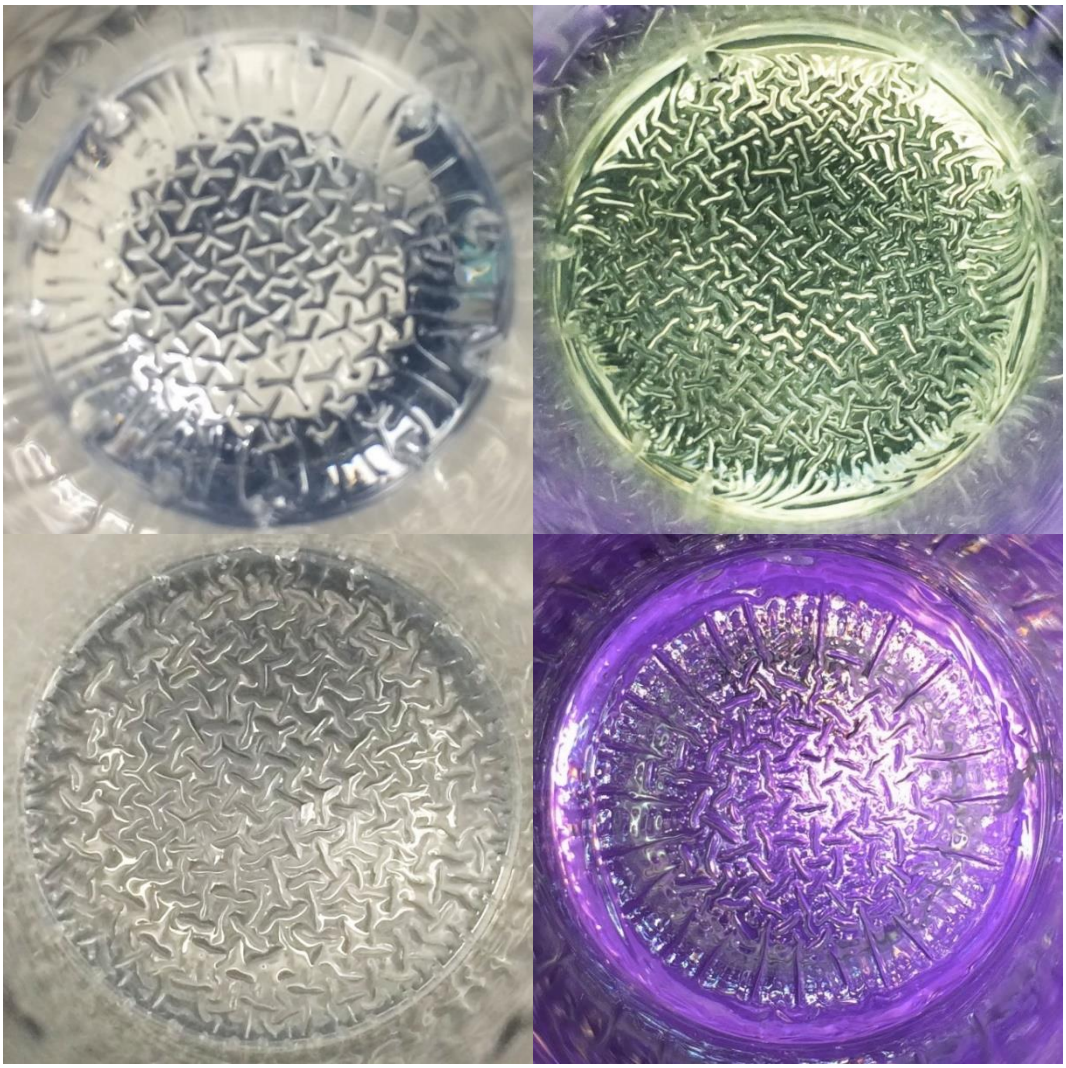

Figure 17. The surface patterns of the PAAm gel samples with the same dimension.

Figure 18. The surface patterns of PAAm gel samples with different dimensions.

The wave-like edges of SWCNTs/PAAm hybrid gels

When fabricating the SWCNTs/PAAm hybrid gels, the edge of the hybrid gels presented wave-like curves that had never been observed on neat PAAm gels when they were taken out of the vials (Figure 19). The phenomenon only occurred when the SWCNTs were well-dispersed. It is inferred that this phenomenon is related to the homogeneity of the aqueous dispersion of SWCNTs and resulted from the incorporation of SWCNTs and the addition of NaDDBS because they are the only two variables in the experiment. There are no researchers that have ever reported such a phenomenon. The mechanism for the formation of the wave-like edge is to be further investigated.

Figure 19. The wave-like edges on the top surface of hybrid gel samples were formed after gelation.

The adhesiveness of hydrogel fragments

Adhesive hydrogels have excellent potential for manufacturing organic and dermatological patches, underwater adhesion and so on.[42–44] When we picked up a piece of fractured samples of SWCNTs/PAAm hybrid gels or neat PAAm gels with tweezers, it was noticed that the piece of fractured gels tightly stuck to the tip (Figure 20). The bond

between the tweezers and the gels was so intense that only violent shake or vibration could separate them. It is interesting that the smooth surfaces of fractured gels are not adhesive at all. The tweezers can only stick to some parts of the ridges of the pieces. Figure 20 shows that a thin film existed between the tweezers and fractured pieces of gels, which withstood hundred or thousand times of its weight. The reasons for the adhesiveness only existing on the ridges of fractured hydrogels are unclear and call for more studies.

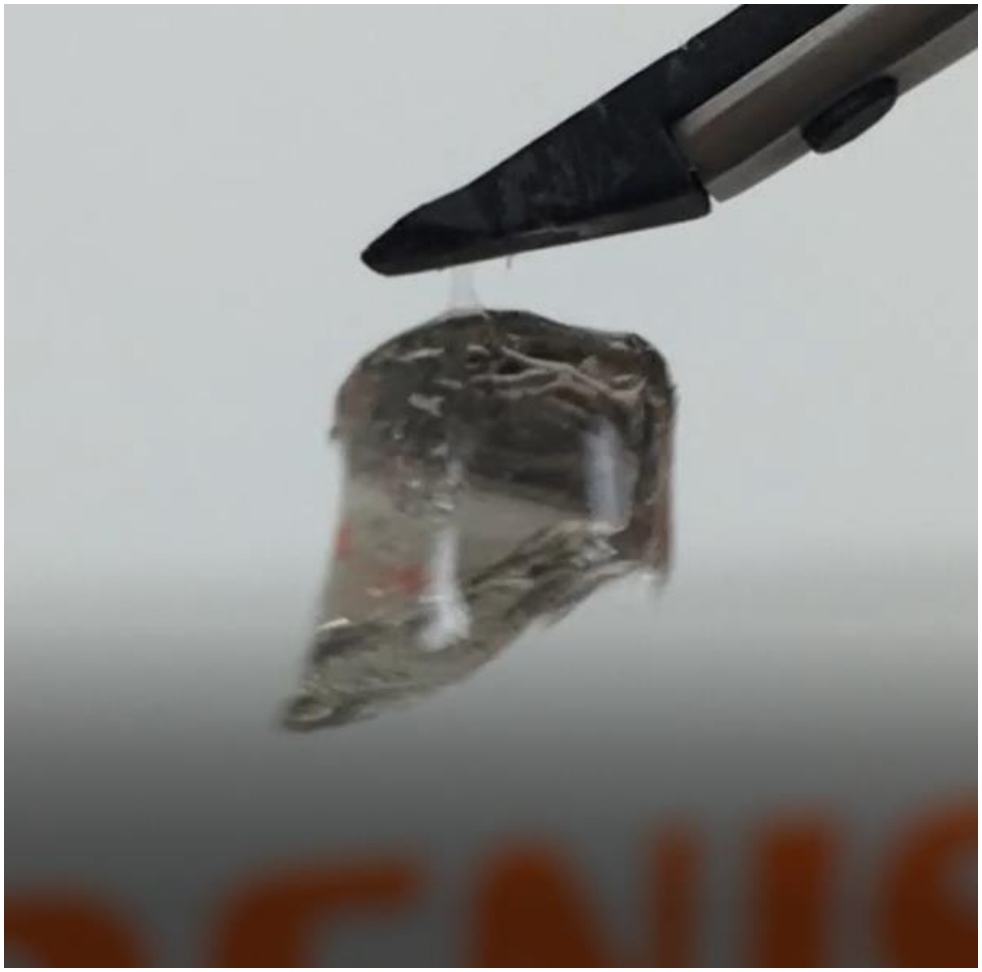

Figure 20. A piece of PAAm hydrogel fragment stuck to tweezers by adhesion.

Conclusions and Future Works

The dispersion of SWCNTs with favorable homogeneity had been successfully prepared. The aqueous dispersion of SWCNTs at a concentration of 0.5 mg/ml remained stable and homogeneous after two months. The SWCNTs/PAAm hybrid gels had subsequently been fabricated via free radical polymerization. The compression tests demonstrated the fusion of PAAm and SWCNTs substantially enhanced the compressive modulus, fracture stress, toughness. The fracture stress and compressive modulus of SWCNTs/PAAm hybrid gels with 0.5 mg/ml SWCNTs increased by 60% and 300% respectively compared with neat PAAm gels. Two specimens of hybrid gels were captured with exceptional fracture stress as high as 1 MPa and fracture strain at 0.98 respectively. The more thoroughly fractured hybrid gels and SEM images of increased micro-networks in the pore structure of the hybrid gels can be used to account for the toughening mechanism. Some phenomena observed in the experiment such as surface patterns, wave-like edges, strong adhesiveness were also discussed.

Although the SWCNTs/PAAm hybrid gels display a significant leap in mechanical strength, it is still not comparable with real soft tissues. Their inherently notch-sensitive quality also hasn't been widely improved. To further enhance the mechanical strength of hydrogels, we will prepare SWCNTs/PAAm hybrid gels with a higher concentration of SWCNTs. Different nano-fibers such as boron nitride nanotubes will also be used to fabricate other nanocomposite hydrogels in the expectation of finding out the finest reinforcing nano-materials for hydrogels. We will also look into the

phenomena observed in the experiment and understand the mechanism behind them.

Reference

(1) Wichterle, O.; LíM, D. Hydrophilic Gels for Biological Use. *Nature* 1960, *185* (4706), 117–118.

(2) Chen, G.; Wang, Y.; Huang, J.-L. Breast Cancer Following Polyacrylamide Hydrogel Injection for Breast Augmentation: A Case Report. *Mol. Clin. Oncol.* 2016, *4* (3), 433–435.

(3) Stashak, T. S.; Farstvedt, E.; Othic, A. Update on Wound Dressings: Indications and Best Use. *Clin. Tech. Equine Pract.* 2004, *3* (2), 148–163.

(4) Hoare, T. R.; Kohane, D. S. Hydrogels in Drug Delivery: Progress and Challenges. *Polymer* 2008, *49* (8), 1993–2007.

(5) Sannino, A.; Demitri, C.; Madaghiele, M. Biodegradable Cellulose-Based Hydrogels: Design and Applications. *Materials* 2009, *2* (2), 353–373.

(6) Bortolin, A.; Aouada, F. A.; Mattoso, L. H. C.; Ribeiro, C. Nanocomposite PAAm/Methyl Cellulose/Montmorillonite Hydrogel: Evidence of Synergistic Effects for the Slow Release of Fertilizers. *J. Agric. Food Chem.* 2013, *61* (31), 7431–7439.

(7) Shin, S. R.; Bae, H.; Cha, J. M.; Mun, J. Y.; Chen, Y.-C.; Tekin, H.; Shin, H.; Farshchi, S.; Dokmeci, M. R.; Tang, S.; et al. Carbon Nanotube Reinforced Hybrid Microgels as Scaffold Materials for Cell Encapsulation. *ACS Nano* 2012, *6* (1), 362–372.

(8) Liu, M.; Zeng, X.; Ma, C.; Yi, H.; Ali, Z.; Mou, X.; Li, S.; Deng, Y.; He, N. Injectable Hydrogels for Cartilage and Bone Tissue Engineering. *Bone Res.* 2017, *5*, 17014.

(9) Patras, G.; Qiao, G. G.; Solomon, D. H. Novel Cross-Linked Homogeneous Polyacrylamide Gels with Improved Separation Properties: Investigation of the Cross-Linker Functionality. *Electrophoresis* 2001, *22* (20), 4303–4310.

(10) Gong, J. P. Why Are Double Network Hydrogels so Tough? *Soft Matter* 2010, *6* (12), 2583.

(11) Okumura, Y.; Ito, K. The Polyrotaxane Gel: A Topological Gel by Figure-of-Eight Cross-Links. *Adv. Mater.* 2001, *13* (7), 485–487.

(12) Parlato, M.; Reichert, S.; Barney, N.; Murphy, W. L. Poly(Ethylene Glycol) Hydrogels with Adaptable Mechanical and Degradation Properties for Use in Biomedical Applications. *Macromol. Biosci.* 2014, *14* (5), 687–698.

(13) Normand, V.; Lootens, D. L.; Amici, E.; Plucknett, K. P.; Aymard, P. New Insight into Agarose Gel Mechanical Properties. *Biomacromolecules* 2000, *1* (4), 730–738.

(14) Pal, S. Mechanical Properties of Biological Materials. In *Design of Artificial Human Joints & Organs*; Springer US: Boston, MA, 2014; pp 23–40.

(15) Liu, Z.; Yang, Z.; Luo, Y. Swelling, PH Sensitivity, and Mechanical Properties of Poly(Acrylamide-Co-Sodium Methacrylate) Nanocomposite Hydrogels Impregnated with Carboxyl-Functionalized Carbon Nanotubes. *Polym. Compos.* 2012, *33* (5), 665–674.

(16) Chatterjee, S.; Lee, M. W.; Woo, S. H. Enhanced Mechanical Strength of Chitosan Hydrogel Beads by Impregnation with Carbon Nanotubes. *Carbon* 2009, *47* (12), 2933–2936.

(17) Wang, S.-F.; Shen, L.; Zhang, W.-D.; Tong, Y.-J. Preparation and Mechanical Properties of Chitosan/Carbon Nanotubes Composites. *Biomacromolecules* 2005, *6* (6), 3067–3072.

(18) Dong, W.; Huang, C.; Wang, Y.; Sun, Y.; Ma, P.; Chen, M. Superior Mechanical Properties of Double-Network Hydrogels Reinforced by Carbon Nanotubes without Organic Modification. *Int. J. Mol. Sci.* 2013, *14* (11), 22380–22394.

(19) Shin, S. R.; Jung, S. M.; Zalabany, M.; Kim, K.; Zorlutuna, P.; Kim, S. bok; Nikkhah, M.; Khabiry, M.; Azize, M.; Kong, J.; et al. Carbon-Nanotube-Embedded Hydrogel Sheets for Engineering Cardiac Constructs and Bioactuators. *ACS Nano* 2013, *7* (3), 2369–2380.

(20) Carbon Nanotube. *Wikipedia*; 2018.

(21) Girifalco, L. A.; Hodak, M.; Lee, R. S. Carbon Nanotubes, Buckyballs, Ropes, and a Universal Graphitic Potential. *Phys. Rev. B* 2000, *62* (19), 13104–13110.

(22) González-Sáiz, J. M.; Pizarro, C. Polyacrylamide Gels as Support for Enzyme Immobilization by Entrapment. Effect of Polyelectrolyte Carrier, PH and Temperature on Enzyme Action and Kinetics Parameters. *Eur. Polym. J.* 2001, *37* (3), 435–444.

(23) Sairam, M.; Babu, V. R.; Vijaya, B.; Naidu, K.; Aminabhavi, T. M. Encapsulation Efficiency and Controlled Release Characteristics of Crosslinked Polyacrylamide Particles. *Int. J. Pharm.* 2006, *320* (1–2), 131–136.

(24) Soppimath, K. S.; Kulkarni, A. R.; Aminabhavi, T. M. Chemically Modified Polyacrylamide-g-Guar Gum-Based Crosslinked Anionic Microgels as PH-Sensitive

Drug Delivery Systems: Preparation and Characterization. *J. Control. Release Off. J. Control. Release Soc.* 2001, *75* (3), 331–345.

(25) Yang, T.-H. New Approaches to the Formation of a Stationary Phase in an Immunoadsorption Wall. *Artif. Organs* 2005, *29* (2), 178–182.

(26) Zhao, H.; Liang, W. A Novel Comby Scaffold with Improved Mechanical Strength for Bone Tissue Engineering. *Mater. Lett.* 2017, *194*, 220–223.

(27) Matarredona, O.; Rhoads, H.; Li, Z.; Harwell, J. H.; Balzano, L.; Resasco, D. E. Dispersion of Single-Walled Carbon Nanotubes in Aqueous Solutions of the Anionic Surfactant NaDDBS. *J. Phys. Chem. B* 2003, *107* (48), 13357–13367.

(28) Cavitation. *Wikipedia*; 2018.

(29) *Encyclopedia of Chemical Technology. Suppl. Vol: Aerogels to Xylylene Polymers*, 4. ed.; Kroschwitz, J. I., Howe-Grant, M., Kirk, R. E., Othmer, D. F., Eds.; A Wiley-Interscience publication; Wiley: New York, NY, 1998.

(30) Ultrasonic Cavitation in Liquids https://www.hielscher.com/cavitat.htm (accessed Apr 26, 2018).

(31) How to disperse CNTs | How to Disperse Carbon Nanotubes | Short MWCNTs | Short MWNTS | Graphitized MWCNTs | Graphitized MWNTs http://www.us-nano.com/how_to_disperse_cnts (accessed Apr 26, 2018).

(32) Thostenson, E.; Li, C.; Chou, T. Nanocomposites in Context. *Compos. Sci. Technol.* 2005, *65* (3–4), 491–516.

(33) Hu, X.; Liu, J.; He, Q.; Meng, Y.; Cao, L.; Sun, Y.-P.; Chen, J.; Lu, F. Aqueous Compatible Boron Nitride Nanosheets for High-Performance Hydrogels. *Nanoscale* 2016, *8* (7), 4260–4266.

(34) Menter, P. Acrylamide Polymerization — A Practical Approach. 8.

(35) Filleter, T.; Bernal, R.; Li, S.; Espinosa, H. D. Ultrahigh Strength and Stiffness in Cross-Linked Hierarchical Carbon Nanotube Bundles. *Adv. Mater.* 2011, *23* (25), 2855–2860.

(36) Buenger, D.; Topuz, F.; Groll, J. Hydrogels in Sensing Applications. *Prog. Polym. Sci.* 2012, *37* (12), 1678–1719.

(37) Bastide, J.; Leibler, L. Large-Scale Heterogeneities in Randomly Cross-Linked Networks. *Macromolecules* 1988, *21* (8), 2647–2649.

(38) Furukawa, H.; Horie, K.; Nozaki, R.; Okada, M. Swelling-Induced Modulation of Static and Dynamic Fluctuations in Polyacrylamide Gels Observed by Scanning Microscopic Light Scattering. *Phys. Rev. E* 2003, *68* (3).

(39) Denisin, A. K.; Pruitt, B. L. Tuning the Range of Polyacrylamide Gel Stiffness for Mechanobiology Applications. *ACS Appl. Mater. Interfaces* 2016, *8* (34), 21893–21902.

(40) Tanaka, T.; Sun, S.-T.; Hirokawa, Y.; Katayama, S.; Kucera, J.; Hirose, Y.; Amiya, T. Mechanical Instability of Gels at the Phase Transition. *Nature* 1987, *325* (6107), 796–798.

(41) Guvendiren, M.; Yang, S.; Burdick, J. A. Swelling-Induced Surface Patterns in Hydrogels with Gradient Crosslinking Density. *Adv. Funct. Mater.* 2009, *19* (19), 3038–3045.

(42) Bioinspired Adhesive Hydrogel Driven by Adenine and Thymine https://pubs.acs.org/doi/pdf/10.1021/acsami.7b04832 (accessed May 1, 2018).

(43) Bradley, L. C.; Bade, N. D.; Mariani, L. M.; Turner, K. T.; Lee, D.; Stebe, K. J. Rough Adhesive Hydrogels (RAd Gels) for Underwater Adhesion. *ACS Appl. Mater. Interfaces* 2017, *9* (33), 27409–27413.

(44) Baït, N.; Grassl, B.; Benaboura, A.; Derail, C. Tailoring the Adhesion Properties of Polyacrylamide-Based Hydrogels. Application for Skin Contact. *J. Adhes. Sci. Technol.* 2013, *27* (9), 1032–1047.